Article

Current Biology

Periodic attention deficits after frontoparietal lesions provide causal evidence for rhythmic attentional sampling

Highlights

- Frontoparietal lesions cause time-specific behavior deficits tied to brain rhythms
- Lesion-induced high-amplitude, low-frequency brain activity impacts behavior
- Theta sampling relies on prefrontal areas and alpha/beta sampling on parietal regions
- The functional architecture of attention is inherently rhythmic

Authors

Isabel Raposo, Sara M. Szczepanski, Kathleen Haaland, Tor Endestad, Anne-Kristin Solbakk, Robert T. Knight, Randolph F. Helfrich

Correspondence

randolph.helfrich@gmail.com

In brief

Focal brain lesions in the frontoparietal network increase low-frequency activity and give rise to a periodic attention deficit where specific moments in time are neglected. Raposo et al. provide causal evidence for the hypothesis that attentional sampling is supported by synchronized oscillatory brain activity in the frontoparietal network.

Raposo et al., 2023, Current Biology *33*, 1–12
November 20, 2023
https://doi.org/10.1016/j.cub.2023.09.065

CellPress

Please cite this article in press as: Raposo et al., Periodic attention deficits after frontoparietal lesions provide causal evidence for rhythmic attentional sampling, Current Biology (2023), https://doi.org/10.1016/j.cub.2023.09.065

Current Biology

CellPress

Article

Periodic attention deficits after frontoparietal lesions provide causal evidence for rhythmic attentional sampling

Isabel Raposo,[1,2] Sara M. Szczepanski,[3] Kathleen Haaland,[4] Tor Endestad,[5,6] Anne-Kristin Solbakk,[5,6,7,8] Robert T. Knight,[3] and Randolph F. Helfrich[1,9,*]

[1]Hertie Institute for Clinical Brain Research, University Medical Center Tübingen, 72076 Tübingen, Germany
[2]International Max Planck Research School for the Mechanisms of Mental Function and Dysfunction, University of Tübingen, Tübingen, Germany
[3]Department of Psychology and the Helen Wills Neuroscience Institute, UC Berkeley, Berkeley, CA 94720, USA
[4]Department of Psychiatry and Behavioral Sciences, University of New Mexico Health Sciences, Albuquerque, NM 87102, USA
[5]Department of Psychology, University of Oslo, 0373 Oslo, Norway
[6]RITMO Centre for Interdisciplinary Studies in Rhythm, Time, and Motion, University of Oslo, 0371 Oslo, Norway
[7]Department of Neurosurgery, Oslo University Hospital, 0372 Oslo, Norway
[8]Department of Neuropsychology, Helgeland Hospital, 8656 Mosjøen, Norway
[9]Lead contact
*Correspondence: randolph.helfrich@gmail.com
https://doi.org/10.1016/j.cub.2023.09.065

SUMMARY

Contemporary models conceptualize spatial attention as a blinking spotlight that sequentially samples visual space. Hence, behavior fluctuates over time, even in states of presumed "sustained" attention. Recent evidence has suggested that rhythmic neural activity in the frontoparietal network constitutes the functional basis of rhythmic attentional sampling. However, causal evidence to support this notion remains absent. Using a lateralized spatial attention task, we addressed this issue in patients with focal lesions in the frontoparietal attention network. Our results revealed that frontoparietal lesions introduce periodic attention deficits, i.e., temporally specific behavioral deficits that are aligned with the underlying neural oscillations. Attention-guided perceptual sensitivity was on par with that of healthy controls during optimal phases but was attenuated during the less excitable sub-cycles. Theta-dependent sampling (3–8 Hz) was causally dependent on the prefrontal cortex, while high-alpha/low-beta sampling (8–14 Hz) emerged from parietal areas. Collectively, our findings reveal that lesion-induced high-amplitude, low-frequency brain activity is not epiphenomenal but has immediate behavioral consequences. More generally, these results provide causal evidence for the hypothesis that the functional architecture of attention is inherently rhythmic.

INTRODUCTION

Attention is a key cognitive function to overcome the brain's limited processing capacities by enhancing behaviorally relevant information.[1,2] Numerous neuroimaging and lesion studies confirm the frontoparietal network as the neural basis of attention.[3–7] Although once viewed as a "static spotlight,"[8] recent research suggests that attention behaves as a "blinking spotlight," sequentially sampling behaviorally relevant spatial locations.[9,10] It remains unaddressed whether a blinking spotlight constitutes an active mechanism to distribute limited cognitive resources or whether its discrete nature is the direct consequence of the inherently waxing and waning nature of brain activity. It has been demonstrated that attention cycles as a function of the underlying neuronal rhythm (~3–12 Hz) of the frontoparietal attention network.[9–15] Performance peaked during phases of enhanced perceptual sensitivity, which are interleaved with suboptimal phases of diminished perceptual sensitivity where attention is shifting to a different location. Although there is mounting correlative evidence, to date there is no causal evidence that demonstrates an unequivocal link between frequency- and spatially specific rhythmic brain activity and the observed rhythmic modulation of attention.

In recent decades, extensive research has studied spatial attention deficits resulting from lesions, particularly in cases of right parietal cortex (PCtx) lesions, as seen in hemispatial neglect.[16–18] Spatial neglect is characterized by a failure to attend to and perceive the contralesional hemifield. However, it has long been recognized that focal lesions in the attention network are also detrimental to sustained attention, i.e., deficits in maintaining attention over several seconds to minutes.[6,19,20] Electrophysiological correlates of attention network lesions are often found in early sensory processing, resulting in reduced amplitudes of processing negativity and P300 event-related potential (ERP).[21,22] However, it is a well-established clinical finding that focal high-amplitude, low-frequency rhythmic brain activity, as observed on scalp electroencephalography (EEG), is indicative of a lesion.[23–26] To date, no study has investigated the

Please cite this article in press as: Raposo et al., Periodic attention deficits after frontoparietal lesions provide causal evidence for rhythmic attentional sampling, Current Biology (2023), https://doi.org/10.1016/j.cub.2023.09.065

effects of frontoparietal lesions on the fine-grained temporal dynamics of attention at the behavioral and electrophysiological level. Furthermore, it remains unclear whether the lesion-induced focal slowing of brain activity has immediate functional consequences.[27]

In this study, we addressed these unanswered questions by combining whole-head EEG recordings with a well-established task probing attention on the rapid timescale of (sub-cycle) oscillatory brain activity. To establish causal links between attention network nodes and rhythmic sampling, we assessed participants with focal lesions in either the prefrontal cortex (PFC) or PCtx, as well as age-matched healthy controls. We tested whether lesions disrupt the temporal organization of the attention network, altering rhythmic sampling behavior. We further assessed whether lesions in different network nodes exhibit distinct spectral signatures, reflecting unique functional contributions to the sequential sampling of the environment. Based on the well-known spatial distribution of brain oscillations,[28,29] we predicted that prefrontal lesions would impair rhythmic sampling in the theta band (~3–8 Hz),[9,30] while parietal lesions should disrupt perceptual alpha/beta-band sampling (~8–14 Hz).[9,31]

RESULTS

We recorded 64-channel EEG from patients with chronic focal lesions in either the lateral PFC or PCtx, none of which exhibited hemispatial neglect, to assess their contributions to rhythmic attentional sampling. Twenty-five patients with unilateral focal lesions (PFC: n = 13, 6 left/7 right, 57 ± 9 years; PCtx: n = 12, 6 left/6 right, 67 ± 21 years; mean ± SD) and 23 age-matched healthy controls completed a lateralized spatial attention task (Figure 1A) that elicits rhythmic sampling behavior.[14] Participants were cued to covertly attend either the left or right visual field and respond to a target after a variable cue-target interval (random onset between 1,000 and 2,000 ms).[14,32,33]

We considered three possible scenarios for how insults to the frontoparietal attention network could impact behavior on a fine-grained temporal scale (Figure 1B): lesions could disrupt the network and either (1) attenuate or (2) abolish the rhythmic sampling. These scenarios imply that rhythmic sampling might constitute a process that coordinates the distribution of limited processing resources across time. However, when assuming that rhythmic behavioral sampling directly stems from underlying rhythmic brain activity, then lesion-induced, low-frequency activity could (3) result in an increase in rhythmic attentional sampling. Alternative scenarios that would yield a comparable pattern, as outlined in scenario 3 (Figure 2A), would entail the lapse of control processes following a lesion, which could possibly release rhythmic sampling processes. Alternatively, this pattern might be observed as a result of a compensatory strategy to mitigate perceptual deficits through enhanced rhythmic sampling. Here, we combined detailed behavioral testing with whole-head EEG to disentangle these possible scenarios.

Focal lesions in the frontoparietal network increase rhythmic attentional sampling

Both age-matched controls and patients (Figures 1C and S1A) performed the lateralized spatial attention task with high accuracy, i.e., responded to cued targets and withheld their response to non-cued targets (Figure 1D, top; controls: 99.53% ± 0.57%; patients: 99.16% ± 0.71%, mean ± SEM; $t_{44} = 1.92$, $p = 0.0606$, $d = 0.57$; two-tailed t test). Moreover, mean reaction times (RTs) did not differ (Figure 1D, center; $t_{44} = -1.24$, $p = 0.2199$, $d = -0.37$; controls 555 ± 83 ms, patients 587 ± 90 ms, mean ± SEM), while RT variance was increased in patients (Figure 1D, bottom; $t_{44} = -2.60$, $p = 0.0126$, $d = -0.77$; controls 14 ± 11 ms, patients 27 ± 20 ms, mean ± SEM). Increased RT variance was present in both PFC and PCtx lesion groups (PFC: $t_{32} = -1.82$, $p = 0.0391$, $d = -0.64$; PCtx $t_{31} = -2.89$, $p = 0.0035$, $d = -1.05$; one-tailed t test) and did not differ between them ($t_{23} = -1.31$, $p = 0.2041$, $d = -0.52$). This effect was independent of the lesioned hemisphere (Figure S1B). The observation of systematically increased RT variance in lesion patients raised the question of whether this increase exhibited a consistent temporal structure. To address this, we assessed RTs as a function of the cue-target interval (Figure 1E; all trials within a 50-ms moving window were averaged, the window was shifted in steps of 1 ms to account for the overall number of trials in patient studies; see also Helfrich et al.[14]).

To quantify the frequency and oscillatory power, we spectrally decomposed the behavioral traces. We removed the 1/f contribution to obtain a whitened power spectrum. First, we considered all available trials. Cluster-based permutation testing revealed narrow-banded power increases in patients in the theta (Figure 1F, top; 2–7 Hz: $p_{cluster} = 0.0079$, $d = -0.80$) and in the high-alpha/low-beta band (12–16 Hz: $p_{cluster} = 0.0125$, $d = -0.74$). To control for a possible impact of eye movements, the analysis was repeated after excluding all trials that contained eye movements, which strengthened the initial observation (Figure 1F, center; note the increase in effect size: 2–7 Hz: $p_{cluster} = 0.0051$, $d = -0.89$; 12–16 Hz: $p_{cluster} = 0.0152$, $d = -0.83$). Increased rhythmic attentional theta- and high-alpha/low-beta-sampling was observed in both patient groups independently (Figure 1F, bottom; PFC: 2–8 Hz: $p_{cluster} = 0.0057$, $d = -1.23$; 10–16 Hz: $p_{cluster} = 0.0057$, $d = -0.92$; PCtx: 2–5 Hz: $p_{cluster} = 0.0311$, $d = -0.85$; 12–16 Hz: $p_{cluster} = 0.0199$, $d = -0.91$). Increased power was present, regardless of whether the stimuli were presented in the ipsilesional or contralesional hemifield (all uncorrected $p > 0.2655$; Figure S1C). To determine the impact of lesion size, we correlated lesion size (number of voxels), and behavioral power across frequencies. This analysis indicated that lesion size was not correlated with behavioral power ($p_{cluster} = 0.1508$). Collectively, these behavioral findings strongly support the hypothesis that a lesion in the frontoparietal network increases rhythmic attentional sampling (cf. scenario 3; Figure 1B).

Increased rhythmic attentional sampling in lesion patients is phase dependent

We next sought to determine the temporal evolution of the elevated rhythmic sampling. We conceived three scenarios based on the behavioral result in the frequency domain to explain the observed spectral pattern in the time domain (Figure 2A). (1) Patients exhibit a similar mean but an overall increased oscillatory amplitude, implying that patients respond faster or slower than controls, depending on the oscillatory phase. (2) Patients respond slightly slower (non-significant offset), albeit with overall stronger fluctuations. In this scenario, patients would perform to par with controls during optimal phases but worse at suboptimal time

Please cite this article in press as: Raposo et al., Periodic attention deficits after frontoparietal lesions provide causal evidence for rhythmic attentional sampling, Current Biology (2023), https://doi.org/10.1016/j.cub.2023.09.065

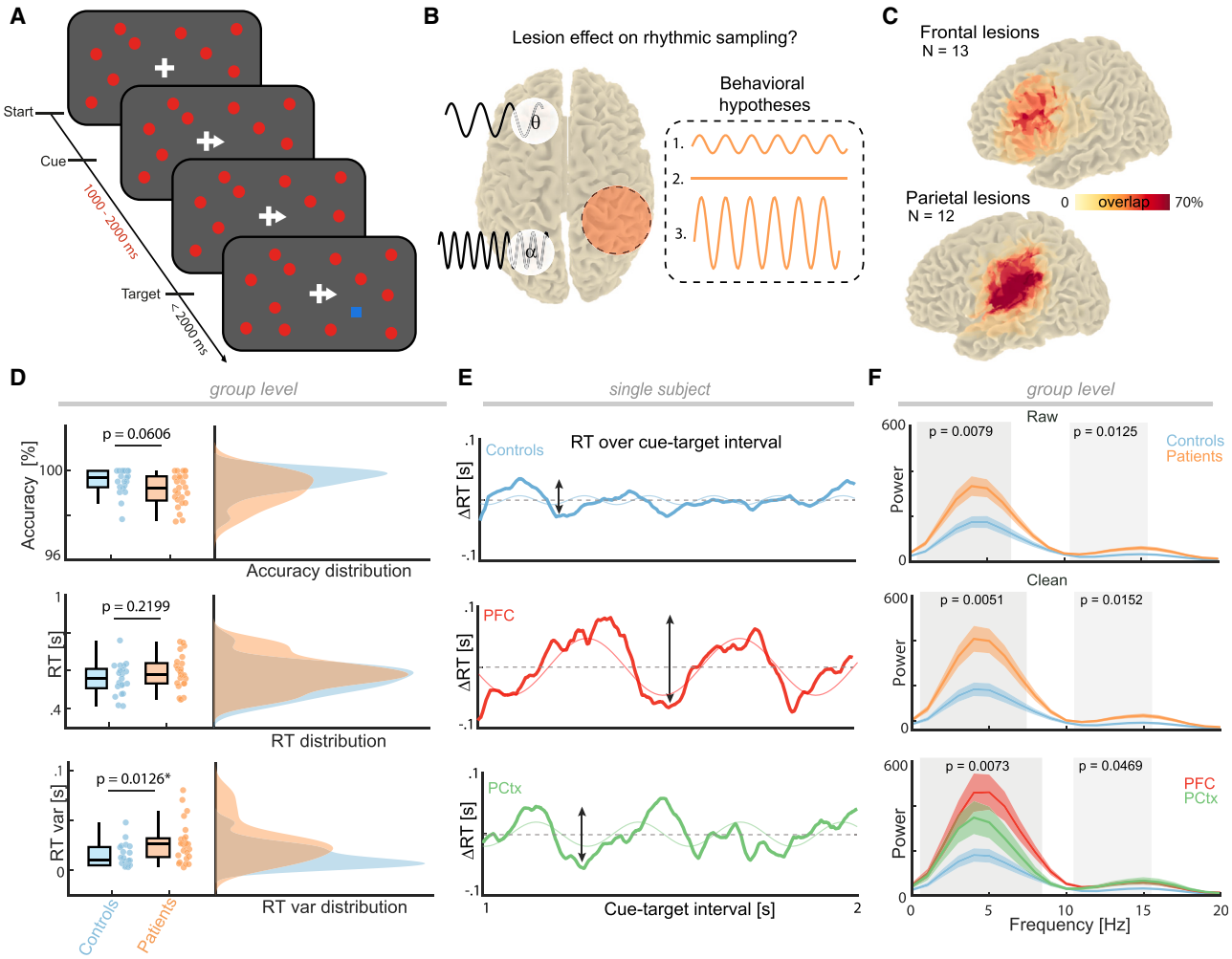

Figure 1. Focal lesions of the frontoparietal network increase rhythmic attentional sampling

(A) Illustration of task design. Participants fixated a central fixation cross on a dynamic background with several visual distractors randomly switched on or off (red, no rhythmicity). A centrally presented spatial cue indicated with high probability (70%) the hemifield participants should covertly attend to. After a variable cue-target interval (1,000–2,000 ms) a target (blue square) appeared, and participants responded with a button press if the target appeared in the cued hemifield.

(B) Hypothesized task outcomes. The prefrontal cortex (PFC) is associated with theta-dependent attention allocation and the parietal cortex (PCtx) is linked to the alpha/beta-band activity. We predicted that a disruption of the frontoparietal network could lead to one of three possible frequency-specific behavioral scenarios: attenuated rhythmic behavioral fluctuations (amplitude decrease), abolishment of rhythmic sampling, or an increased rhythmic sampling (amplitude increase).

(C) Lesion reconstruction: PFC and PCtx lesion overlapped (in %) for all 25 patients (13 PFC, 12 PCtx) normalized to the left hemisphere. See Figure S1 for single subjects.

(D) Accuracy, reaction time (RT) and RT variance per group (whiskers indicate maximum and minimum, dots correspond to individual participants). Age-matched controls (blue) and patients (orange) only differed in reaction time variance, with larger variability in the patients.

(E) Demeaned, time-resolved RTs and model fit (unconstrained sine wave, thin line) as a function of the cue-target interval for one exemplary participant per group (controls, blue; PFC, red; PCtx, green).

(F) Group-level 1/f-corrected power spectra of the behavioral time courses. Top: patients exhibited a frequency-specific increase in rhythmic attentional sampling in the theta (2–7 Hz, $d = -0.80$) and high-alpha/low-beta band (12–16, $d = -0.74$). Center: this effect became more pronounced after exclusion of eye movements (2–7 Hz, $d = -0.89$; 12–16 Hz, $d = -0.83$). Bottom: the increased amplitude in the theta and alpha/beta band was present in both patient groups.

points. (3) When both offset and amplitude increase, then patients should perform worse at both optimal and suboptimal phases as compared with healthy controls. To test which scenario best explained the behavioral results, we compared the worst and best RT of every participant, as well as the mean and the amplitude, in the raw behavioral traces (Figures 2B and S2).

Mean RTs did not differ between the groups (Figure 1D, center; $t_{44} = -1.24$, $p = 0.2199$, $d = -0.37$). To test the predictions of the different scenarios, we employed a mixed repeated-measures ANOVA with *group* (controls vs. patients) as between-subject variable and *phase* (best vs. worst) as within-subject variable (Figure 2C). Performance between groups did not differ significantly ($F_{1,44} = 1.70$, $p = 0.199$, $\eta^2_p = 0.04$; thus, replicating and extending Figure 1D), highlighting that, irrespective of phase, accuracy was comparable. We observed a significant effect of the factor *phase* ($F_{1,44} = 271.3$, $p < 0.001$, $\eta^2_p = 0.86$), which was

Please cite this article in press as: Raposo et al., Periodic attention deficits after frontoparietal lesions provide causal evidence for rhythmic attentional sampling, Current Biology (2023), https://doi.org/10.1016/j.cub.2023.09.065

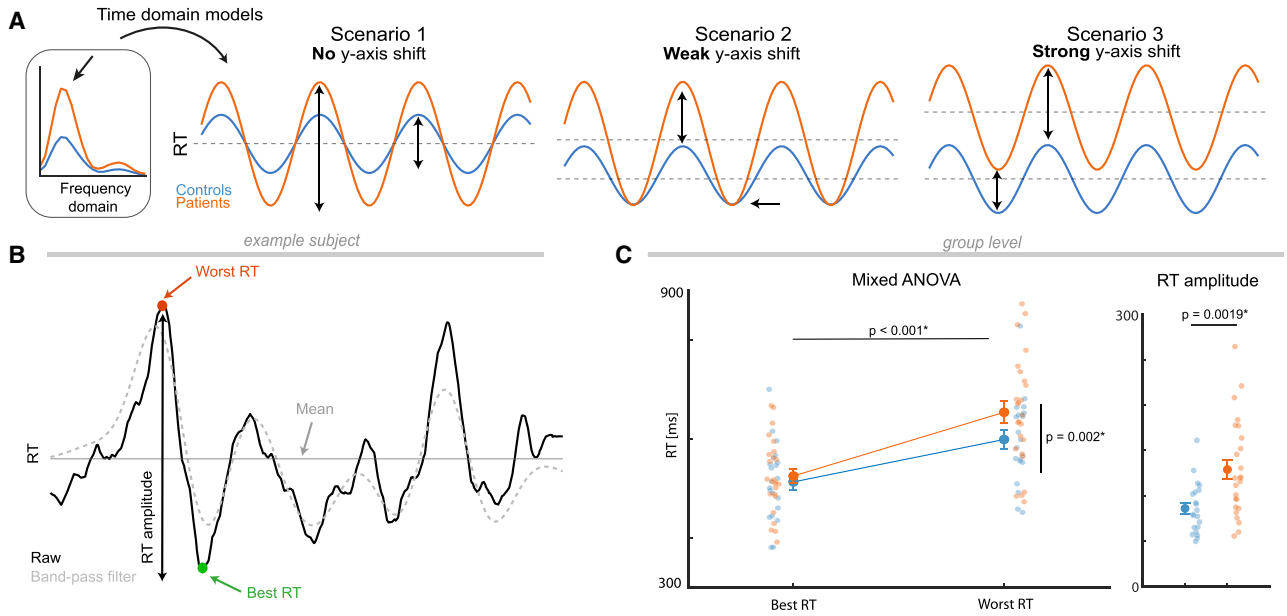

Figure 2. Scenario comparison of the temporal evolution of behavioral deficits in lesion patients

(A) Schematic of hypothesized behavioral scenarios underlying increased rhythmic sampling. Three scenarios were conceivable; scenario 1: comparable mean but increased variance (amplitude), implying that patients (orange) should exhibit faster RTs at optimal phases and slower RTs during less favorable phases compared with controls (blue). Scenario 2: different mean (non-significant offset along the y axis) and increased amplitude. Hence, behavioral performance in patients should be on par with controls during optimal phases but significantly worse during suboptimal phases. Scenario 3: different mean, increased amplitude. Hence, performance at optimal and suboptimal phases should be worse in patients.

(B) Behavioral time course of one representative patient. Points of interest are defined on the raw (solid line) and band-pass filtered traces (dashed line, Figure S2). We defined (1) mean, (2) amplitude, and (3) best behavior, as well as (4) worst behavior in the time domain.

(C) Repeated-measures ANOVA was performed to investigate the effects of *group* (between-subjects) and *phase* (within-subject). No main effect of *group* ($p = 0.199$), but a significant main effect of *phase* ($p < 0.001$) as well as a significant interaction effect of *phase* × *group* ($p = 0.002$) were detected. Consequently, RT amplitude was significantly increased in patients ($p = 0.0019$). Collectively, these observations support model 2.

expected, given that the data were grouped according to best and worst RT. Critically, we observed a significant interaction between *phase* × *group* ($F_{1,44} = 10.9$, $p = 0.002$, $\eta^2_p = 0.20$). As indicated in Figure 2C, this significant interaction was driven by the key prediction that was common to all three scenarios, namely that performance is decreased during the worst phase ($t_{44} = -1.83$, $p = 0.0369$, $d = -0.54$; one-tailed t test). As a control, we also tested the group difference for the best RT bin and did not observe a significant difference ($t_{44} = -0.53$, $p = 0.7026$, $d = -0.16$). As a direct result of the significant interaction, we observed that the RT amplitude was increased ($t_{44} = -3.30$ $p = 0.0019$, $d = -0.98$; two-tailed t test; Figure 2C, right). Collectively, these observations support the predictions of scenario 2 and establish temporally specific behavioral deficits in patients suffering from chronic cortical lesions.

These behavioral results make several specific predictions regarding the underlying neurophysiology. (1) Given that the patients performed the task with high accuracy, we hypothesized that indices of sensory processing, i.e., early evoked responses, remain largely intact. (2) High-amplitude, low-frequency EEG activity is indicative of an underlying cortical lesion,[24,25] which might predict the enhanced amplitude in rhythmic behavioral sampling. (3) We observed a clear distinction into best and worst phases in both patients and controls, implying that phase-behavior relationships are maintained following a lesion. (4) Lastly, our behavioral results suggest that theta rhythmic sampling is stronger in PFC patients, while high-alpha/low-beta-band sampling is stronger in PCtx patients (Figure 1F), indicating that the PFC is the main source driving theta activity, while high-alpha/low-beta dominates in parietal areas.

Focal lesions increase low-frequency activity in the frontoparietal network

We first assessed cue-locked and target-locked ERPs and observed that ERPs were similar in both groups (Figure 3A; smallest $p_{cluster} = 0.2038$). We replicated the previously reported attenuation of early components in PFC lesion patients in the ipsilesional hemisphere[34] (Figure 3B; $t_{12} = 2.69$, $p = 0.0197$, $d = 0.45$). This ipsilesional attenuation was not observed in the PCtx group ($t_{11} = 0.22$, $p = 0.8267$, $d = 0.03$), was significantly different between the patient groups ($t_{23} = 2.17$, $p = 0.0408$, $d = 0.87$), and was temporally specific (see Figure S3A for P300 analysis). Critically, we did not observe any group differences during the behaviorally relevant cue-target interval (1–2 s).

In addition, we observed a well-known clinical finding, with channels over the lesioned tissue displaying high-amplitude, low-frequency activity (Figure 3C). To quantify this observation, we spectrally decomposed the electrophysiological time series during the cue-target interval. We observed increased power in the low-frequency range (1–16 Hz) across the majority of EEG sensors in patients (Figure S3B, left; $p_{cluster} = 0.0259$,

Please cite this article in press as: Raposo et al., Periodic attention deficits after frontoparietal lesions provide causal evidence for rhythmic attentional sampling, Current Biology (2023), https://doi.org/10.1016/j.cub.2023.09.065

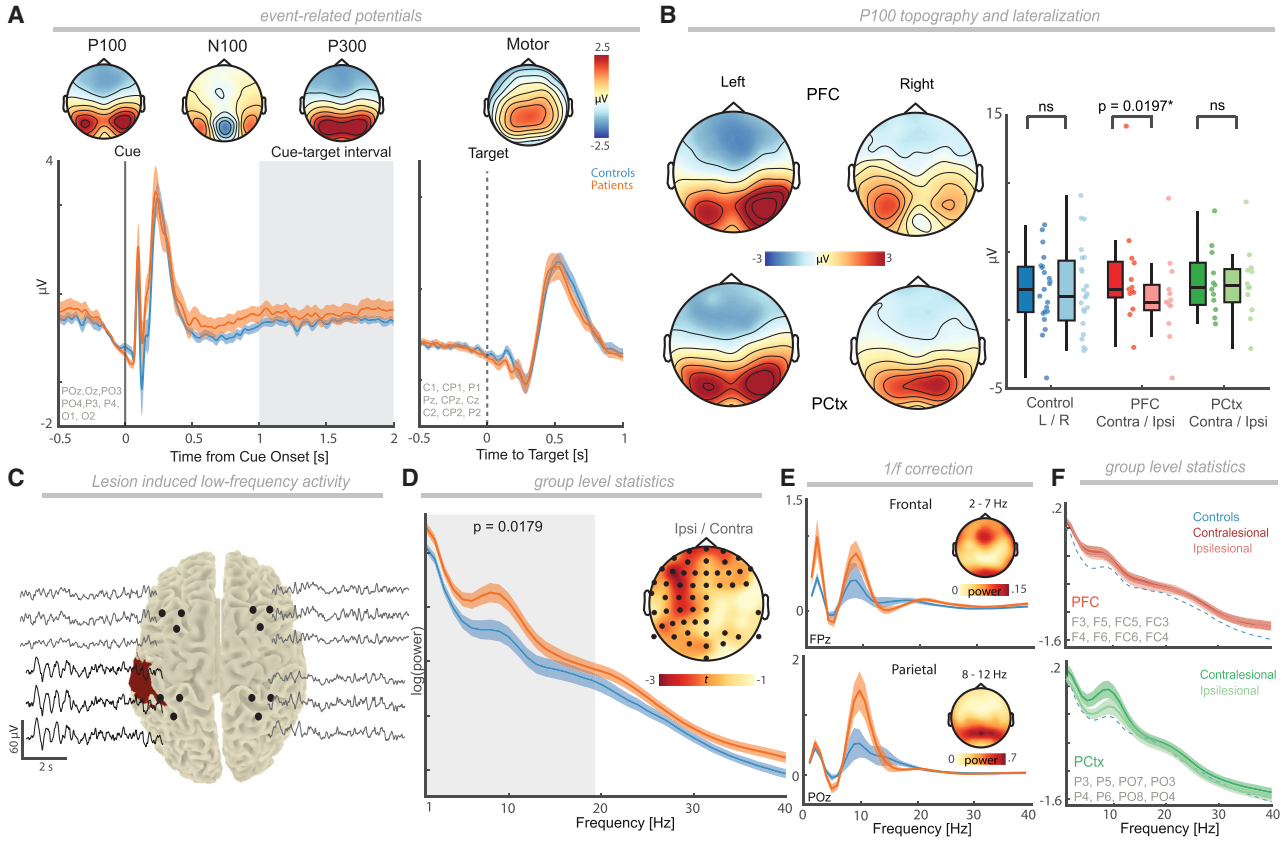

Figure 3. Focal lesions increase low-frequency activity in the frontoparietal attention network

(A) Grand-average event-related potentials (ERPs, mean ± SEM), cue- (left, posterior channels), and target-locked ERP (right, central channels) demonstrate that ERPs did not differ between patients (orange) and controls (blue). Topographies of the main ERPs (P100, N100, P300, and motor response) averaged across all subjects.

(B) Left: P100 topography for PFC and PCtx patients with either a lesion in the left or right hemisphere. Right: mean P100 ERP (80–110 ms) per group (contra- vs. ipsilesional posterior channels). Activity over ipsilateral posterior channels was attenuated in PFC lesion patients.

(C) Illustration of increased perilesional, low-frequency EEG activity.

(D) Grand-average power spectra with mirrored electrodes in right hemisphere lesion patients to the left (mean ± SEM, black dots indicate significant channels; Figure S3B for non-mirrored electrode positioning). Patients exhibited widespread increased low-frequency power in comparison with controls (1–19 Hz; $p_{cluster}$ = 0.0179).

(E) 1/f-corrected power spectrum after irregular resampling. Distinct theta and alpha peaks were evident. Theta activity was more pronounced over frontal regions (upper panel; inset depicts band-limited spectral power topography), while alpha/low beta activity exhibited a peak over parietooccipital sensors (lower panel). Note that 1/f-corrected oscillatory power was enhanced in patients in a region-specific manner.

(F) Upper panel: grand-average power spectra of contra- and ipsilesional PFC channels, revealing no significant differences. Blue dashed line highlights the mean of the control group. Lower: PCtx group. Same conventions as in the upper panel.

d = −0.58). To determine whether this power increase was pronounced over the lesioned hemisphere, we mirrored all the electrodes across the midline, which again revealed a large bihemispheric cluster (Figure 3D; 1–19 Hz; $p_{cluster}$ = 0.0179, d = −0.55). We also re-referenced the EEG signal to a unipolar reference not overlaying the lesions (Cz). This again replicated a widespread increase in lower-frequency activity in patients (Figure S3B, right; $p_{cluster}$ = 0.0149, d = −0.49). To separate oscillatory activity from broadband 1/f activity, we employed irregular resampling auto-spectral analysis,[35] which revealed distinct regionally specific oscillatory signatures over frontal and parietal EEG sensors (Figure 3E). Finally, we compared activity at ipsi- and contralesional electrodes. Both PFC and PCtx lesions resulted in a comparable, widespread power increase (Figure 3F; all uncorrected p > 0.0965). In sum, these findings demonstrate a widespread increase of low-frequency EEG activity in lesion patients.

Theta and high-alpha/low-beta oscillations predict increased rhythmic attentional sampling

After observing systematic increased low-frequency activity in both behavior (Figure 1F) and electrophysiology (Figure 3D) in patients, we tested whether these increments were directly correlated. In the control group, mean behavioral and EEG power were significantly positively correlated across lower frequencies, with two distinct peaks at 4 and 11 Hz (Figure 4A, left; 1–20 Hz: rho = 0.507, $p_{cluster}$ = 0.0110; cluster-corrected correlations).

Please cite this article in press as: Raposo et al., Periodic attention deficits after frontoparietal lesions provide causal evidence for rhythmic attentional sampling, Current Biology (2023), https://doi.org/10.1016/j.cub.2023.09.065

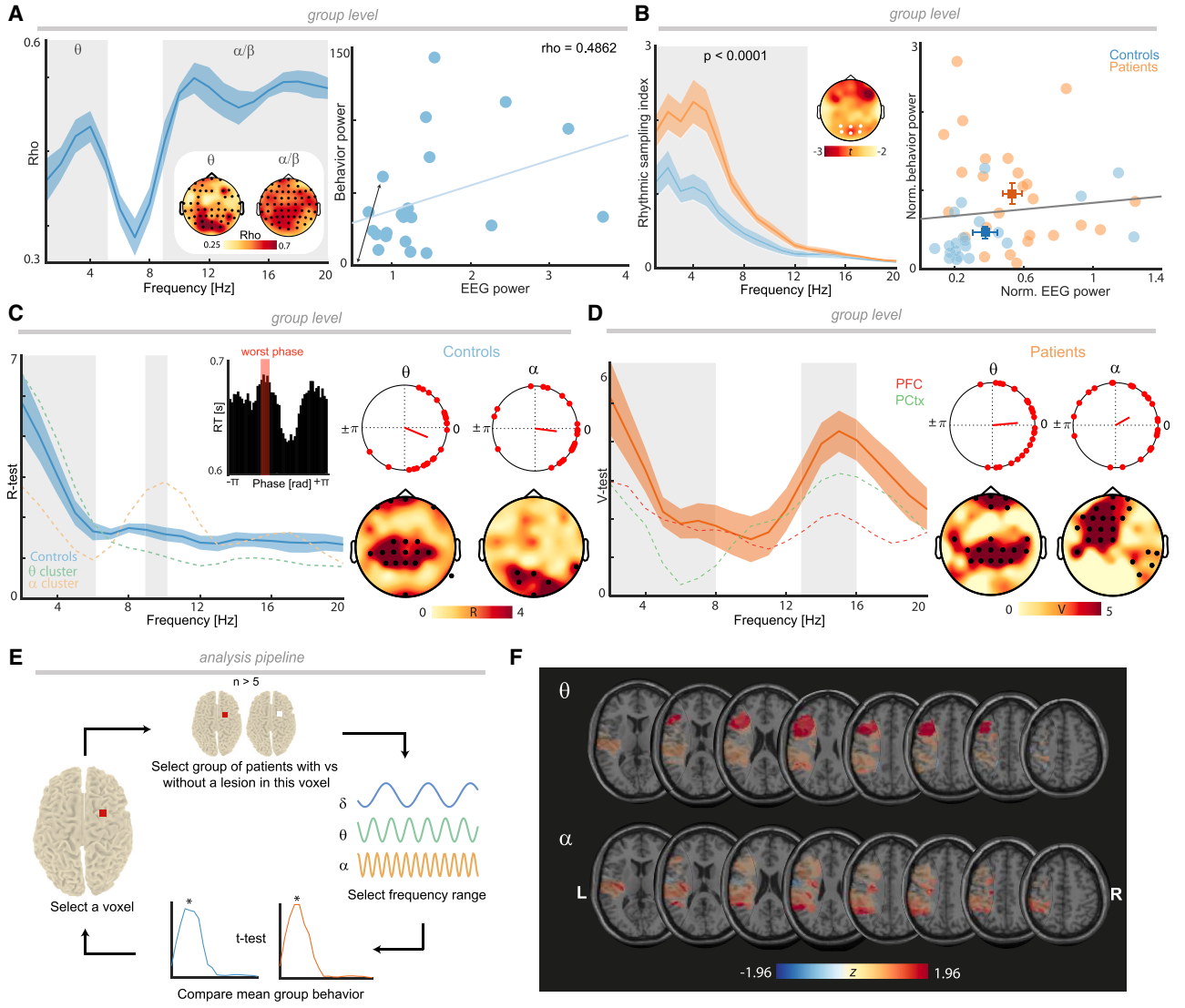

Figure 4. Neuronal oscillations predict rhythmic attentional sampling

(A) Left: correlation of spectrally resolved behavior and electrophysiology in healthy controls ($p_{cluster}$ = 0.0110; shaded error bars indicate bootstrapped correlation coefficient error, 100 repetitions; gray shaded areas; thresholded at **rho** = 0.3). Inset: topographies indicate the spatial extent (black dots indicate cluster electrodes). Right: correlation of neural theta power and behavioral power (averaged across all significant theta cluster channels; the blue line highlights the linear regression). To quantify the relationship of EEG and behavioral power, we calculated the rhythmic sampling index (the magnitude of the black arrow after normalization).

(B) Left: patients had an increased association between behavioral and EEG power in lower frequencies (1–13 Hz, $p < 0.0001$). Right: normalized EEG power as a function of normalized behavioral power for healthy participants (squares, mean; error bars, SEM).

(C) Left: phase-resolved behavior as a function of frequency in healthy controls to assess whether the phase that was associated with worst performance (cf. Figure 2A; *model 2*) was consistent at the group level. The inset demonstrates the phase-resolved reaction times in the theta range (single subject electrode example). Rayleigh tests identified consistent phase clustering in the theta (2–6 Hz) and alpha (9–10 Hz) range (gray shaded areas depict significant frequencies, FDR-corrected $p < 0.05$; shaded error bars indicate SEM across channels; dashed lines indicate the within-cluster average; cf. right panels). Right: spatial extent of the phase clustering in the theta- and alpha-bands. Significant theta-phase consistency was observed over fronto-centro-parietal sensors, while alpha phase consistency was observed over occipital sensors.

(D) Left: phase-behavior relationships remained stable in lesion patients. We observed a highly comparable mean direction (V test; cf. C) in patients in the theta (2–8 Hz) and high-alpha/low-beta band (13–16 Hz; FDR corrected, $p < 0.05$; dashed lines represent the mean test statistic V of PFC and PCtx patients). Significant phase clustering in the same direction as healthy controls indicates that the non-uniform relationship between phase and behavior persisted after focal lesions. Right: spatial extent of the phase clustering.

(E) Illustration of the spectrally resolved voxel-based lesion-symptom mapping (VLSM) analysis.

(F) VLSM maps depict *z* values of all ($p < 0.05$, uncorrected) voxels in the theta (2–7 Hz) and high-alpha/low-beta (12–16 Hz range, frequency range analogous to Figure 1F). See Figure S4 for FDR-corrected maps. Lesions within the lateral prefrontal cortex predicted a behavioral theta power increase, whereas parietal deficits predicted an increase in rhythmic sampling in the alpha band.

Please cite this article in press as: Raposo et al., Periodic attention deficits after frontoparietal lesions provide causal evidence for rhythmic attentional sampling, Current Biology (2023), https://doi.org/10.1016/j.cub.2023.09.065

We repeated the same analysis in the patient group, but did not observe a significant cluster at $p < 0.05$, which was a direct result of the frequency-specific differences between both patient groups, as outlined below. However, we observed distinct peaks in the theta (6 Hz) and alpha/beta band (12 Hz). Hence, we computed cluster-based correlation separately for the PFC and PCtx lesion patients (Figure S4A). In PFC lesion patients, we observed a significant correlation (6–12 Hz: mean rho = 0.497, $p_{cluster} = 0.0410$), particularly over frontoparietal channels. In contrast, no significant cluster was identified in PCtx patients at $p < 0.05$. However, the results indicated a positive correlation between rhythmic EEG activity and rhythmic sampling in the posterior electrode cluster (cf. Figure 4B) in the high-alpha/low-beta range (12–13 Hz: mean rho = 0.597, $p_{uncorrected} \leq 0.0042$).

To further quantify the relationship between behavioral and EEG activity in patients, we introduced a composite metric to quantify their mutual dependence for every subject, channel, and frequency. The rhythmic sampling index (RSI) was defined as the resultant vector length in a two-dimensional (2D) space spanned by frequency-specific behavior and EEG power (Figure 4A, right). Patients exhibited a larger RSI in comparison with controls in the lower-frequency range (Figure 4B, left; 1–13 Hz: $p_{cluster} < 0.0001$, $d = -0.7283$), indicating that patients' larger neural oscillation's amplitude predict larger behavioral oscillatory power (Figure 4B, right). To control for the possibility that the larger RSI in patients was driven by extreme values along one of the axes, we calculated the angle (relative to the x axis; bounded between 0° and 90°) for every observation per subject, channel, and frequency and compared it between controls and patients. We observed that the mean angle did not differ between groups (no cluster observed, all $p > 0.05$). A comparable angle between behavior and EEG power suggests that the index was not conflated by extreme values along one of the axes.

Phase dependence of rhythmic attentional sampling is preserved in patients

Having established that a lesion-induced increase of low-frequency EEG activity predicts an increase in rhythmic attentional sampling in behavior, we next tested a key prediction of scenario 2 (Figure 2A), which implies that the precise oscillatory phase that governs behavior should be consistent in controls and patients. Specifically, we determined the suboptimal phase where the slowest RT occurred. To quantify the association between oscillatory phase and behavior, we computed phase-resolved RTs (Figure 4C, left). We divided the phase into 50 equally distributed bins (from $-\pi$ to $+\pi$) and computed the average RT for all trials within a 90° window. The suboptimal phase (slowest RT) was then determined for every subject per channel and frequency. To test for phase clustering per frequency, we first conducted Rayleigh tests in healthy controls for each channel and frequency, separately. We observed significant phase clustering in the theta range (Figure 4C; 2–6 Hz; −24.9° ± 10.1°, circular mean ± SEM; resultant vector length $r = 0.64$, Rayleigh $z = 3.21$, false discovery rate [FDR]-corrected all $p \leq 0.0075$) and alpha band (9–10 Hz; −7.4° ± 11.8°, circular mean ± SEM; resultant vector length $r = 0.51$, Rayleigh $z = 2.16$, FDR-corrected all $p \leq 0.0215$). Next, we assessed whether patients exhibited the same preferred phase as controls (non-uniform phase distribution around the mean phase in healthy controls; V test). We observed significantly similar phase clustering in the theta (Figure 4D; 2–8 Hz; 5.2° ± 10.2°, circular mean ± SEM, $v = 3.08$, FDR-corrected all $p \leq 0.0075$) and high-alpha/low-beta bands (13–16 Hz; 29.4° ± 12.8°, circular mean ± SEM, $v = 4.33$, FDR-corrected all $p \leq 0.0059$), thus suggesting that phase-behavior relationships in patients remained intact. This finding was further corroborated by additional Watson-Wilson tests (circular ANOVA) for theta ($F_{1, 46} = 3.18$, $p = 0.0812$) and high-alpha/low-beta ($F_{1,46} = 2.56$, $p = 0.1167$). In sum, these results establish that a clear separation into optimal and suboptimal phases was maintained after focal lesions. These findings reveal that the increased rhythmic attentional sampling is not a consequence of altered phase-behavior dependencies.

Dissociable neural origins of theta- and high-alpha/low-beta-band rhythmic sampling

Lastly, we determined how different nodes of the frontoparietal network contributed to the theta- and high-alpha/low-beta-band rhythmic attentional sampling. We employed spectrally resolved voxel-based lesion symptom mapping (VLSM; Figures 4E and 4F) to assess the contribution of every voxel to frequency-specific rhythmic behavior. We observed that the theta behavioral cluster was associated with lesions in the lateral PFC (Figure 4F, thresholded at $z = \pm 1.96$; 2–8 Hz; $d = 1.00$, see Figure S4 for FDR-corrected maps), while the high-alpha/low-beta behavioral cluster was associated with lesions in the temporoparietal junction (12–16 Hz; $d = 1.11$). Collectively, spectrally resolved VLSM provides causal evidence for the hypothesis that theta-dependent rhythmic attentional sampling originates in the PFC, while high-alpha/low-beta-band sampling originates from parietal regions.

DISCUSSION

Our results demonstrate that chronic lesions in the human frontoparietal attention network cause periodic attention deficits, where patients exhibit temporally specific behavioral deficits on the rapid timescale of neural oscillations. The current findings reveal that lesion-induced high-amplitude, low-frequency brain activity is not epiphenomenal, but has immediate functional consequences on attention. Although patients performed on par with controls during optimal phases, attention allocation was attenuated during suboptimal time windows. These results causally support the hypothesis that low-frequency oscillations underlie rhythmic environmental sampling[2] and, more broadly, reveal their causal role for the rhythmic nature of cognition.[36]

A rhythmic theory of attention

Classic theories conceptualized attention as a static spotlight that prioritizes perception at an attended location[8] or object[37] and has its neural basis in the frontoparietal network.[3] However, recent findings challenge this traditional view,[11,14,38,39] revealing dynamic fluctuations in spatial attention at a theta rhythm (3–8 Hz)[10] when examined at a finer temporal scale. Recently, similar observations have been made for object-,[11] feature-based,[40] and cue-guided visual attention.[13] It might also apply to working memory[41] or other sensory domains, such as audition.[42] Several lines of inquiry suggested that rhythmic brain

Please cite this article in press as: Raposo et al., Periodic attention deficits after frontoparietal lesions provide causal evidence for rhythmic attentional sampling, Current Biology (2023), https://doi.org/10.1016/j.cub.2023.09.065

activity in the frontoparietal attention network constitutes a viable mechanism that efficiently segregates attentional sampling from attentional shifting.[2] Electrophysiological recordings in non-human primates[12,43] and humans[14,44] have demonstrated that theta oscillations shape neural excitability and periodically reweight functional connections between different frontoparietal nodes.[12,44,45] Recently, the rhythmic nature of attention has been called into question, based on behavioral modeling,[46] and is now actively debated.[47,48] These controversial findings are a direct consequence of the lack of causal data linking rhythmic fluctuations in behavior to oscillatory brain activity.

Here, we provide causal evidence by studying patients with focal lesions in the attention network. We employed the same task used recently to demonstrate theta-phase dependence on behavior, even at relatively long stimulus-onset asynchronies (SOAs). It is currently unknown for how long attentional rhythmic cycles persist after cue presentation. Our results revealed increased rhythmic attentional sampling in lesion patients. Although both PFC and PCtx patients exhibited increased sampling in the theta and high-alpha/low-beta bands, VLSM localized theta-band sampling to the PFC and high-alpha/low-beta-band sampling to the PCtx.[45,49–54] Following a lesion, low-frequency-band activity increased in the immediate proximity of the focal insult (Figure 3D), which mediated pronounced rhythmic attentional sampling in a spatially and frequency-specific manner (Figures 4B and 4F). These results are compatible with the initial hypothesis (scenario 3) that the increase in rhythmic sampling might be the consequence of elevated low-frequency activity (Figures 4B and 4F). Although the relationship of increased EEG and behavioral rhythmic activity constitutes the most parsimonious explanation, it is important to consider alternative interpretations. For example, increased rhythmic sampling could stem from a release of rhythmic sampling in other nodes. This idea aligns with our findings that oscillatory power was also increased contralateral to the lesion (Figures 3D–3F). Although we observed elevated theta and alpha/beta behavioral sampling in both lesion groups (Figure 1F), we found the most pronounced correlations between behavior and frequency-specific EEG activity in immediate lesion proximity (Figures 4F and S4A), and primarily at the locally dominant frequency (Figure 3E). These observations suggest that the increased rhythmic sampling does not simply reflect a release of frontal attention sampling. Because all patients suffered from chronic lesions, it is furthermore conceivable that elevated rhythmic sampling could constitute a compensatory strategy to counteract perceptual deficits. Again, the spatial specificity of the observed relationship between behavior and EEG activity in immediate proximity to the lesion does not strongly support this consideration. Similarly, there is currently no evidence that rhythmic sampling reflects a voluntary process[2] at the fast timescale of theta/alpha or beta oscillations (<200 ms), reinforcing the notion that enhanced rhythmic sampling constitutes an involuntary process.

Collectively, these results align with the hypothesis that enhanced rhythmic sampling might be driven by increased amplitude, where the oscillatory organization into excitatory and inhibitory sub-cycles is preserved following focal lesions (Figure 4D). Future studies aimed at disentangling perceptual from attention-related sampling are needed to understand whether and how top-down control processes (re-) structure rhythmic attentional sampling after a focal insult. Ideally, these studies will consider patients in the acute (hours/days), semi-chronic (day/weeks), and chronic (months/years) disease stages to study the temporal evolution and to capture compensatory effects.

Attention deficits in space and time after focal brain lesions

Attention deficits upon focal lesions have mainly been studied in the spatial domain and are best exemplified by the hemispatial neglect syndrome.[16,55] Typically, spatial neglect is caused by inferior parietal lesions in the right hemisphere,[56] affecting mostly the contralesional visual field, but bilateral effects have also been described.[57–59] Moreover, spatial neglect can be observed after cortical or subcortical lesions[17,60,61] and occasionally also affects the ipsilesional visual field.[55,59] In contrast to a clear division of labor between the right and left hemisphere that is essential for visual perception or oculomotor behavior, we observed that focal insults to any hemisphere and network node give rise to comparable behavioral effects (Figures 1F, S1B, and S1C). This observation suggests that rhythmic attentional sampling does not arise from inter-hemispheric competition but may rather arise from a precisely tuned, cooperative interplay in the bihemispheric frontoparietal network. This raises the question of how the interplay between different network nodes on both hemispheres is organized. One likely possibility is that the thalamus may orchestrate cortical networks,[62] as demonstrated in non-human primates.[45] Future studies that combine thalamic and cortical recordings could unravel whether and how the thalamus structures inter-hemispheric interactions in a spatially and frequency-specific manner.

Neglect is often pronounced in the (semi-) acute phase[32] and has been shown to be time-dependent, albeit on longer timescales than reported here. For instance, the attentional blink[63] was markedly prolonged to ~1,400 ms (as compared with ~400 ms) in neglect patients.[64] Likewise, neglect patients exhibit aberrant inhibition-of-return, with facilitation rather than inhibition for repeated events on the non-neglected hemifield.[65,66] Although time-dependent attention deficits over several seconds have been described in neglect patients[63–65] and the causal role of the parietal lobe in temporal attention has been demonstrated,[67] no work has examined attention deficits on the fine-grained temporal scale of brain oscillations.

In this study, patients did not exhibit spatial neglect (Figure S1B). However, behavioral deficits were evident as increased response time variability, consistent with previous reports in frontal lesion patients,[68,69] which had not been linked to electrophysiological brain activity. Critically, the increased variability exhibited a clear temporal structure with distinct spectral peaks in the theta and high-alpha/low-beta bands when probed on a fine-grained temporal scale. These frequency- and phase-specific deficits were defined by the lesion-mediated, increased low-frequency EEG amplitude.

Collectively, these observations reveal a periodic attention deficit, characterized by diminished perception at specific time intervals that align with the inhibitory sub-cycle of low-frequency oscillations. As in spatial neglect, our results demonstrate that deficits emerge after lesions to multiple network nodes, hence, conceptualizing periodic attention deficit as a network disorder.

Brain lesions and EEG slowing

Focal EEG slowing is a well-established clinical hallmark of underlying brain lesions,[23–26] but the neural mechanisms responsible for this phenomenon remain unclear. Traditionally regarded as physical distortions caused by the damaged tissue,[70] more recent evidence suggests that low-frequency activity may reflect functional reorganization after stroke.[24,27] The emergence of coherent neural activity might index reorganization and has been shown to predict motor recovery.[27] However, how these findings translate to higher cognitive functions remains unknown. Here, we replicated increased low-frequency amplitude following a focal lesion (Figure 3D). Our findings demonstrate that increased power is not limited to the perilesional cortex (Figures S3B and S3C). Low-frequency power increase also predicted increased behavioral power, i.e., temporally structured response time variability, in a phase-specific manner: during optimal phases, patients performed on par with controls, as previously observed,[57] while behavior was periodically impaired during suboptimal phases. These findings are consistent with previous results demonstrating that the oscillatory phase defines windows of heightened or diminished perceptual abilities and subsequent behavior.[71–73] The impact of phase is markedly pronounced when amplitude is high, as previously exemplified for parietal alpha oscillations.[71,74] Here, we observed a comparable pattern, where the overall organization into optimal and suboptimal oscillatory phases remained intact (Figures 4C and 4D). Interestingly, in our study we observed that during the optimal phase patients performed on par with healthy controls, but significantly worse during the suboptimal phase (Figure 2C). Altogether, these findings establish that coherent, lesion-mediated, low-frequency activity has an immediate behavioral impact and does not constitute an epiphenomenon. A testable hypothesis for future studies is whether the emergence of low-frequency activity is a suitable biomarker to track cognitive recovery, similar to previous findings that implicated low-frequency activity in neural plasticity underlying motor recovery after stroke.[24,27]

Conclusions

In summary, our results reveal a hitherto unknown behavioral deficit resulting from focal brain lesions to the frontoparietal attention network. We demonstrate that lesion-mediated, coherent low-frequency activity introduces a periodic behavioral attention deficit with reduced perception for specific moments in time. Specifically, neglected time windows are defined as a less excitable sub-cycle of the underlying neural oscillation. These results provide causal evidence for the hypothesis that rhythmic attentional sampling has its neural basis in synchronized frontoparietal network activity.[38,45]

STAR★METHODS

Detailed methods are provided in the online version of this paper and include the following:

- KEY RESOURCES TABLE
- RESOURCE AVAILABILITY
  - Lead contact
  - Materials availability
  - Data and code availability
- EXPERIMENTAL MODEL AND SUBJECT DETAILS
  - Participants
- METHOD DETAILS
  - Lesion reconstruction
  - Behavioral task
  - EEG and eye position data acquisition
- QUANTIFICATION AND STATISTICAL ANALYSIS
  - Behavioral data analysis
  - EEG data analysis
  - Spectrally-resolved voxel-based lesion symptom mapping
  - Statistical testing

SUPPLEMENTAL INFORMATION

Supplemental information can be found online at https://doi.org/10.1016/j.cub.2023.09.065.

ACKNOWLEDGMENTS

This work was funded by the Baden Wuerttemberg Foundation (Postdoctoral Fellowship, R.F.H.), German Research Foundation Emmy Noether Program (DFG HE8329/2-1; R.F.H.), the Hertie Foundation Network for Excellence in Clinical Neuroscience (R.F.H.), the Research Council of Norway (grant number 240389; A.-K.S. and T.E.), the Research Council of Norway (Centre of Excellence Scheme, grant number 262762), RITMO (RITPART International Partnerships for RITMO Centre of Excellence, grant number 274996; A.-K.S., T.E., and R.T.K.), Department of Veterans Affairs Research Career Scientist Program (K.H.), and by an NIMH Conte Center Grant (1 PO MH109429; R.T.K.) and NINDS (2 R01 NS021135; R.T.K.).

AUTHOR CONTRIBUTIONS

Conceptualization, R.F.H., R.T.K., and I.R.; methodology, I.R. and R.F.H.; formal analysis, I.R.; investigation, R.F.H., S.M.S., K.H., T.E., and A.-K.S.; resources, R.T.K., K.H., T.E., and A.S.; writing—original draft, I.R.; writing—review and editing, I.R., R.F.H., and R.T.K.; supervision, R.F.H; funding acquisition, R.F.H. and R.T.K.

DECLARATION OF INTERESTS

The authors declare no competing interests.

Received: May 23, 2023
Revised: August 8, 2023
Accepted: September 26, 2023
Published: October 17, 2023

REFERENCES

1. Buschman, T.J., and Kastner, S. (2015). From behavior to neural dynamics: an integrated theory of attention. Neuron *88*, 127–144. https://doi.org/10.1016/j.neuron.2015.09.017.
2. Fiebelkorn, I.C., and Kastner, S. (2019). A rhythmic theory of attention. Trends Cogn. Sci. *23*, 87–101. https://doi.org/10.1016/j.tics.2018.11.009.
3. Corbetta, M., Akbudak, E., Conturo, T.E., Snyder, A.Z., Ollinger, J.M., Drury, H.A., Linenweber, M.R., Petersen, S.E., Raichle, M.E., Van Essen, D.C., et al. (1998). A common network of functional areas for attention and eye movements. Neuron *21*, 761–773. https://doi.org/10.1016/S0896-6273(00)80593-0.
4. Kastner, S., Pinsk, M.A., De Weerd, P., Desimone, R., and Ungerleider, L.G. (1999). Increased activity in human visual cortex during directed attention in the absence of visual stimulation. Neuron *22*, 751–761. https://doi.org/10.1016/s0896-6273(00)80734-5.

5. Knight, R.T. (1984). Decreased response to novel stimuli after prefrontal lesions in man. Electroencephalogr. Clin. Neurophysiol. *59*, 9–20. https://doi.org/10.1016/0168-5597(84)90016-9.

6. Malhotra, P., Coulthard, E.J., and Husain, M. (2009). Role of right posterior parietal cortex in maintaining attention to spatial locations over time. Brain *132*, 645–660. https://doi.org/10.1093/brain/awn350.

7. Petersen, S.E., Robinson, D.L., and Currie, J.N. (1989). Influences of lesions of parietal cortex on visual spatial attention in humans. Exp. Brain Res. *76*, 267–280. https://doi.org/10.1007/BF00247887.

8. Posner, M.I. (1980). Orienting of attention. Q. J. Exp. Psychol. *32*, 3–25. https://doi.org/10.1080/00335558008248231.

9. VanRullen, R. (2016). Perceptual cycles. Trends Cogn. Sci. *20*, 723–735. https://doi.org/10.1016/j.tics.2016.07.006.

10. Landau, A.N., and Fries, P. (2012). Attention samples stimuli rhythmically. Curr. Biol. *22*, 1000–1004. https://doi.org/10.1016/j.cub.2012.03.054.

11. Fiebelkorn, I.C., Saalmann, Y.B., and Kastner, S. (2013). Rhythmic sampling within and between objects despite sustained attention at a cued location. Curr. Biol. *23*, 2553–2558. https://doi.org/10.1016/j.cub.2013.10.063.

12. Fiebelkorn, I.C., Pinsk, M.A., and Kastner, S. (2018). A dynamic interplay within the frontoparietal network underlies rhythmic spatial attention. Neuron *99*, 842–853.e8. https://doi.org/10.1016/j.neuron.2018.07.038.

13. Helfrich, R.F., Huang, M., Wilson, G., and Knight, R.T. (2017). Prefrontal cortex modulates posterior alpha oscillations during top-down guided visual perception. Proc. Natl. Acad. Sci. USA *114*, 9457–9462. https://doi.org/10.1073/pnas.1705965114.

14. Helfrich, R.F., Fiebelkorn, I.C., Szczepanski, S.M., Lin, J.J., Parvizi, J., Knight, R.T., and Kastner, S. (2018). Neural mechanisms of sustained attention are rhythmic. Neuron *99*, 854–865.e5. https://doi.org/10.1016/j.neuron.2018.07.032.

15. Dugué, L., McLelland, D., Lajous, M., and VanRullen, R. (2015). Attention searches nonuniformly in space and in time. Proc. Natl. Acad. Sci. USA *112*, 15214–15219. https://doi.org/10.1073/pnas.1511331112.

16. Heilman, K.M., and Valenstein, E. (1979). Mechanisms underlying hemispatial neglect. Ann. Neurol. *5*, 166–170. https://doi.org/10.1002/ana.410050210.

17. Husain, M., and Kennard, C. (1996). Visual neglect associated with frontal lobe infarction. J. Neurol. *243*, 652–657. https://doi.org/10.1007/BF00878662.

18. Karnath, H.-O., Fruhmann Berger, M., Küker, W., and Rorden, C. (2004). The anatomy of spatial neglect based on voxelwise statistical analysis: a study of 140 patients. Cereb. Cortex *14*, 1164–1172. https://doi.org/10.1093/cercor/bhh076.

19. Rueckert, L., and Grafman, J. (1996). Sustained attention deficits in patients with right frontal lesions. Neuropsychologia *34*, 953–963. https://doi.org/10.1016/0028-3932(96)00016-4.

20. Rueckert, L., and Grafman, J. (1998). Sustained attention deficits in patients with lesions of posterior cortex. Neuropsychologia *36*, 653–660. https://doi.org/10.1016/s0028-3932(97)00150-4.

21. Knight, R.T. (1997). Distributed cortical network for visual attention. J. Cogn. Neurosci. *9*, 75–91. https://doi.org/10.1162/jocn.1997.9.1.75.

22. Knight, R.T., Hillyard, S.A., Woods, D.L., and Neville, H.J. (1981). The effects of frontal cortex lesions on event-related potentials during auditory selective attention. Electroencephalogr. Clin. Neurophysiol. *52*, 571–582. https://doi.org/10.1016/0013-4694(81)91431-0.

23. Allaman, L., Mottaz, A., and Guggisberg, A.G. (2021). Disrupted resting-state EEG alpha-band interactions as a novel marker for the severity of visual field deficits after brain lesion. Clin. Neurophysiol. *132*, 2101–2109. https://doi.org/10.1016/j.clinph.2021.05.029.

24. Cassidy, J.M., Wodeyar, A., Wu, J., Kaur, K., Masuda, A.K., Srinivasan, R., and Cramer, S.C. (2020). Low-frequency oscillations are a biomarker of injury and recovery after stroke. Stroke *51*, 1442–1450. https://doi.org/10.1161/STROKEAHA.120.028932.

25. Fanciullacci, C., Bertolucci, F., Lamola, G., Panarese, A., Artoni, F., Micera, S., Rossi, B., and Chisari, C. (2017). Delta power is higher and more symmetrical in ischemic stroke patients with cortical involvement. Front. Hum. Neurosci. *11*, 385. https://doi.org/10.3389/fnhum.2017.00385.

26. Wu, J., Srinivasan, R., Burke Quinlan, E., Solodkin, A., Small, S.L., and Cramer, S.C. (2016). Utility of EEG measures of brain function in patients with acute stroke. J. Neurophysiol. *115*, 2399–2405. https://doi.org/10.1152/jn.00978.2015.

27. Ramanathan, D.S., Guo, L., Gulati, T., Davidson, G., Hishinuma, A.K., Won, S.J., Knight, R.T., Chang, E.F., Swanson, R.A., and Ganguly, K. (2018). Low-frequency cortical activity is a neuromodulatory target that tracks recovery after stroke. Nat. Med. *24*, 1257–1267. https://doi.org/10.1038/s41591-018-0058-y.

28. Buzsáki, G., and Draguhn, A. (2004). Neuronal oscillations in cortical networks. Science *304*, 1926–1929. https://doi.org/10.1126/science.1099745.

29. Engel, A.K., Fries, P., and Singer, W. (2001). Dynamic predictions: oscillations and synchrony in top–down processing. Nat. Rev. Neurosci. *2*, 704–716. https://doi.org/10.1038/35094565.

30. Jia, J., Liu, L., Fang, F., and Luo, H. (2017). Sequential sampling of visual objects during sustained attention. PLoS Biol. *15*, e2001903. https://doi.org/10.1371/journal.pbio.2001903.

31. Jensen, O., and Mazaheri, A. (2010). Shaping functional architecture by oscillatory alpha activity: gating by inhibition. Front. Hum. Neurosci. *4*, 186.

32. Deouell, L.Y., Sacher, Y., and Soroker, N. (2005). Assessment of spatial attention after brain damage with a dynamic reaction time test. J. Int. Neuropsychol. Soc. *11*, 697–707. https://doi.org/10.1017/S1355617705050824.

33. Szczepanski, S.M., Crone, N.E., Kuperman, R.A., Auguste, K.I., Parvizi, J., and Knight, R.T. (2014). Dynamic changes in phase-amplitude coupling facilitate spatial attention control in fronto-parietal cortex. PLoS Biol. *12*, e1001936. https://doi.org/10.1371/journal.pbio.1001936.

34. Voytek, B., Davis, M., Yago, E., Barceló, F., Vogel, E.K., and Knight, R.T. (2010). Dynamic neuroplasticity after human prefrontal cortex damage. Neuron *68*, 401–408. https://doi.org/10.1016/j.neuron.2010.09.018.

35. Wen, H., and Liu, Z. (2016). Separating fractal and oscillatory components in the power spectrum of neurophysiological signal. Brain Topogr. *29*, 13–26. https://doi.org/10.1007/s10548-015-0448-0.

36. Helfrich, R.F., and Knight, R.T. (2016). Oscillatory dynamics of prefrontal cognitive control. Trends Cogn. Sci. *20*, 916–930. https://doi.org/10.1016/j.tics.2016.09.007.

37. Treisman, A.M., and Gelade, G. (1980). A feature-integration theory of attention. Cogn. Psychol. *12*, 97–136. https://doi.org/10.1016/0010-0285(80)90005-5.

38. Helfrich, R.F., Breska, A., and Knight, R.T. (2019). Neural entrainment and network resonance in support of top-down guided attention. Curr. Opin. Psychol. *29*, 82–89. https://doi.org/10.1016/j.copsyc.2018.12.016.

39. VanRullen, R., Carlson, T., and Cavanagh, P. (2007). The blinking spotlight of attention. Proc. Natl. Acad. Sci. USA *104*, 19204–19209. https://doi.org/10.1073/pnas.0707316104.

40. Re, D., Inbar, M., Richter, C.G., and Landau, A.N. (2019). Feature-based attention samples stimuli rhythmically. Curr. Biol. *29*, 693–699.e4. https://doi.org/10.1016/j.cub.2019.01.010.

41. Chota, S., Leto, C., van Zantwijk, L., and Van der Stigchel, S. (2022). Attention rhythmically samples multi-feature objects in working memory. Sci. Rep. *12*, 14703. https://doi.org/10.1038/s41598-022-18819-z.

42. Zoefel, B., Archer-Boyd, A., and Davis, M.H. (2018). Phase entrainment of brain oscillations causally modulates neural responses to intelligible speech. Curr. Biol. *28*, 401–408.e5. https://doi.org/10.1016/j.cub.2017.11.071.

43. Kienitz, R., Schmiedt, J.T., Shapcott, K.A., Kouroupaki, K., Saunders, R.C., and Schmid, M.C. (2018). Theta rhythmic neuronal activity and

reaction times arising from cortical receptive field interactions during distributed attention. Curr. Biol. *28*, 2377–2387.e5. https://doi.org/10.1016/j.cub.2018.05.086.

44. Landau, A.N., Schreyer, H.M., van Pelt, S., and Fries, P. (2015). Distributed attention is implemented through theta-rhythmic gamma modulation. Curr. Biol. *25*, 2332–2337. https://doi.org/10.1016/j.cub.2015.07.048.

45. Fiebelkorn, I.C., Pinsk, M.A., and Kastner, S. (2019). The mediodorsal pulvinar coordinates the macaque fronto-parietal network during rhythmic spatial attention. Nat. Commun. *10*, 215. https://doi.org/10.1038/s41467-018-08151-4.

46. Brookshire, G. (2022). Putative rhythms in attentional switching can be explained by aperiodic temporal structure. Nat. Hum. Behav. *6*, 1280–1291. https://doi.org/10.1038/s41562-022-01364-0.

47. Vinck, M., Uran, C., and Schneider, M. (2022). Aperiodic processes explaining rhythms in behavior: a matter of false detection or definition?. Preprint at PsyArXiv. https://doi.org/10.31234/osf.io/wzvfh.

48. Tosato, T., Rohenkohl, G., Dowdall, J.R., and Fries, P. (2022). Quantifying rhythmicity in perceptual reports. NeuroImage *262*, 119561. https://doi.org/10.1016/j.neuroimage.2022.119561.

49. Jensen, O., Bonnefond, M., and VanRullen, R. (2012). An oscillatory mechanism for prioritizing salient unattended stimuli. Trends Cogn. Sci. *16*, 200–206. https://doi.org/10.1016/j.tics.2012.03.002.

50. Sadaghiani, S., Scheeringa, R., Lehongre, K., Morillon, B., Giraud, A.L., D'esposito, M., and Kleinschmidt, A. (2012). Alpha-band phase synchrony is related to activity in the fronto-parietal adaptive control network. J. Neurosci. *32*, 14305–14310. https://doi.org/10.1523/JNEUROSCI.1358-12.2012.

51. Lobier, M., Palva, J.M., and Palva, S. (2018). High-alpha band synchronization across frontal, parietal and visual cortex mediates behavioral and neuronal effects of visuospatial attention. NeuroImage *165*, 222–237. https://doi.org/10.1016/j.neuroimage.2017.10.044.

52. Veniero, D., Gross, J., Morand, S., Duecker, F., Sack, A.T., and Thut, G. (2021). Top-down control of visual cortex by the frontal eye fields through oscillatory realignment. Nat. Commun. *12*, 1757. https://doi.org/10.1038/s41467-021-21979-7.

53. Gallotto, S., Duecker, F., Oever, S.T., Schuhmann, T., de Graaf, T.A., and Sack, A.T. (2020). Relating alpha power modulations to competing visuospatial attention theories. NeuroImage *207*, 116429. https://doi.org/10.1016/j.neuroimage.2019.116429.

54. Pietrelli, M., Zanon, M., Làdavas, E., Grasso, P.A., Romei, V., and Bertini, C. (2019). Posterior brain lesions selectively alter alpha oscillatory activity and predict visual performance in hemianopic patients. Cortex *121*, 347–361. https://doi.org/10.1016/j.cortex.2019.09.008.

55. Parton, A., Malhotra, P., and Husain, M. (2004). Hemispatial neglect. J. Neurol. Neurosurg. Psychiatry *75*, 13–21.

56. Vallar, G., and Perani, D. (1986). The anatomy of unilateral neglect after right-hemisphere stroke lesions. A clinical/CT-scan correlation study in man. Neuropsychologia *24*, 609–622. https://doi.org/10.1016/0028-3932(86)90001-1.

57. Battelli, L., Cavanagh, P., Martini, P., and Barton, J.J.S. (2003). Bilateral deficits of transient visual attention in right parietal patients. Brain *126*, 2164–2174. https://doi.org/10.1093/brain/awg221.

58. Battelli, L., Pascual-Leone, A., and Cavanagh, P. (2007). The 'when' pathway of the right parietal lobe. Trends Cogn. Sci. *11*, 204–210. https://doi.org/10.1016/j.tics.2007.03.001.

59. Battelli, L., Cavanagh, P., Intriligator, J., Tramo, M.J., Hénaff, M.A., Michèl, F., and Barton, J.J.S. (2001). Unilateral right parietal damage leads to bilateral deficit for high-level motion. Neuron *32*, 985–995. https://doi.org/10.1016/S0896-6273(01)00536-0.

60. Karnath, H.O., Himmelbach, M., and Rorden, C. (2002). The subcortical anatomy of human spatial neglect: putamen, caudate nucleus and pulvinar. Brain *125*, 350–360. https://doi.org/10.1093/brain/awf032.

61. Vallar, G. (2001). Extrapersonal visual unilateral spatial neglect and its neuroanatomy. NeuroImage *14*, S52–S58. https://doi.org/10.1006/nimg.2001.0822.

62. Halassa, M.M., and Kastner, S. (2017). Thalamic functions in distributed cognitive control. Nat. Neurosci. *20*, 1669–1679. https://doi.org/10.1038/s41593-017-0020-1.

63. Raymond, J.E., Shapiro, K.L., and Arnell, K.M. (1992). Temporary suppression of visual processing in an RSVP task: an attentional blink? J. Exp. Psychol. Hum. Percept. Perform. *18*, 849–860. https://doi.org/10.1037/0096-1523.18.3.849.

64. Husain, M., Shapiro, K., Martin, J., and Kennard, C. (1997). Abnormal temporal dynamics of visual attention in spatial neglect patients. Nature *385*, 154–156. https://doi.org/10.1038/385154a0.

65. Bartolomeo, P., Chokron, S., and Siéroff, E. (1999). Facilitation instead of inhibition for repeated right-sided events in left neglect. NeuroReport *10*, 3353–3357. https://doi.org/10.1097/00001756-199911080-00018.

66. Klein, R.M. (2000). Inhibition of return. Trends Cogn. Sci. *4*, 138–147. https://doi.org/10.1016/S1364-6613(00)01452-2.

67. Agosta, S., Magnago, D., Tyler, S., Grossman, E., Galante, E., Ferraro, F., Mazzini, N., Miceli, G., and Battelli, L. (2017). The pivotal role of the right parietal lobe in temporal attention. J. Cogn. Neurosci. *29*, 805–815. https://doi.org/10.1162/jocn_a_01086.

68. Stuss, D.T., Murphy, K.J., Binns, M.A., and Alexander, M.P. (2003). Staying on the job: the frontal lobes control individual performance variability. Brain *126*, 2363–2380. https://doi.org/10.1093/brain/awg237.

69. MacDonald, S.W.S., Nyberg, L., and Bäckman, L. (2006). Intra-individual variability in behavior: links to brain structure, neurotransmission and neuronal activity. Trends Neurosci. *29*, 474–480. https://doi.org/10.1016/j.tins.2006.06.011.

70. Johnson, E.L., Dewar, C.D., Solbakk, A.-K., Endestad, T., Meling, T.R., and Knight, R.T. (2017). Bidirectional frontoparietal oscillatory systems support working memory. Curr. Biol. *27*, 1829–1835.e4. https://doi.org/10.1016/j.cub.2017.05.046.

71. Mathewson, K.E., Gratton, G., Fabiani, M., Beck, D.M., and Ro, T. (2009). To see or not to see: prestimulus alpha phase predicts visual awareness. J. Neurosci. *29*, 2725–2732. https://doi.org/10.1523/JNEUROSCI.3963-08.2009.

72. Busch, N.A., Dubois, J., and VanRullen, R. (2009). The phase of ongoing EEG oscillations predicts visual perception. J. Neurosci. *29*, 7869–7876. https://doi.org/10.1523/JNEUROSCI.0113-09.2009.

73. Haegens, S., Nácher, V., Luna, R., Romo, R., and Jensen, O. (2011). α-Oscillations in the monkey sensorimotor network influence discrimination performance by rhythmical inhibition of neuronal spiking. Proc. Natl. Acad. Sci. USA *108*, 19377–19382. https://doi.org/10.1073/pnas.1117190108.

74. Hanslmayr, S., Aslan, A., Staudigl, T., Klimesch, W., Herrmann, C.S., and Bäuml, K.H. (2007). Prestimulus oscillations predict visual perception performance between and within subjects. NeuroImage *37*, 1465–1473. https://doi.org/10.1016/j.neuroimage.2007.07.011.

75. Psychology Software Tools, Inc. Soultions for Research, Assessment, and Education (2016). E-Prime 3.0. https://pstnet.com/.

76. The MathWorks Inc. (2021). MATLAB. Version R2021a. https://de.mathworks.com/.

77. Oostenveld, R., Fries, P., Maris, E., and Schoffelen, J.M. (2011). FieldTrip: open source software for advanced analysis of MEG, EEG, and invasive electrophysiological data. Comput. Intell. Neurosci. *2011*, 156869. https://doi.org/10.1155/2011/156869.

78. Berens, P. (2009). CircStat: a MATLAB toolbox for circular statistics. J. Stat. Softw. *31*, 1–21. https://doi.org/10.18637/jss.v031.i10.

79. Penny, W.D., Friston, K.J., Ashburner, J.T., Kiebel, S.J., and Nichols, T.E. (2011). Statistical Parametric Mapping: The Analysis of Functional Brain Images (Elsevier).

80. Martínez-Cagigal, V. (2022). Multiple testing toolbox. https://www.mathworks.com/matlabcentral/fileexchange/70604-multiple-testing-toolbox.

81. VanRullen, R. (2016). How to evaluate phase differences between trial groups in ongoing electrophysiological signals. Front. Neurosci. *10*, 426. https://doi.org/10.3389/fnins.2016.00426.

82. the jamovi project (2023). jamovi. Version 2.3 [Computer Software]. https://www.jamovi.org/.

83. Ashburner, J., and Friston, K.J. (2005). Unified segmentation. NeuroImage *26*, 839–851. https://doi.org/10.1016/j.neuroimage.2005.02.018.

84. Rorden, C., and Brett, M. (2000). Stereotaxic display of brain lesions. Behav. Neurol. *12*, 191–200.

85. Bates, E., Wilson, S.M., Saygin, A.P., Dick, F., Sereno, M.I., Knight, R.T., and Dronkers, N.F. (2003). Voxel-based lesion–symptom mapping. Nat. Neurosci. *6*, 448–450. https://doi.org/10.1038/nn1050.

86. Maris, E., and Oostenveld, R. (2007). Nonparametric statistical testing of EEG- and MEG-data. J. Neurosci. Methods *164*, 177–190. https://doi.org/10.1016/j.jneumeth.2007.03.024.

87. Stouffer, S.A., Suchman, E.A., Devinney, L.C., Star, S.A., and Williams, R.M., Jr. (1949). The American Soldier: Adjustment during Army Life. (Studies in Social Psychology in World War II)*1* (Princeton University Press).

Please cite this article in press as: Raposo et al., Periodic attention deficits after frontoparietal lesions provide causal evidence for rhythmic attentional sampling, Current Biology (2023), https://doi.org/10.1016/j.cub.2023.09.065

STAR★METHODS

KEY RESOURCES TABLE

REAGENT or RESOURCE	SOURCE	IDENTIFIER
Software and algorithms		
EPrime	Psychology Software Tools[75]	https://pstnet.com/; RRID: SCR_009567
MATLAB 2021a	Mathworks[76]	http://www.mathworks.com; RRID: SCR_001622
FieldTrip 20210912	Oostenveld et al.[77]	https://www.fieldtriptoolbox.org/; RRID: SCR_004849
CircStat 2012	Berens[78]	https://www.mathworks.com/matlabcentral/fileexchange/10676-circular-statistics-toolbox-directional-statistics; RRID: SCR_016651
SPM8, SPM12	Penny et al.[79]	https://www.fil.ion.ucl.ac.uk/spm/; RRID: SCR_007037
Multiple Testing Toolbox	Martínez-Cagigal[80]	https://www.mathworks.com/matlabcentral/fileexchange/70604-multiple-testing-toolbox
Phase Opposition Code	VanRullen[81]	https://www.github.com/rufinv/phase-opposition-code
Jamovi 2.3	the jamovi project[82]	https://www.jamovi.org; RRID: SCR_016142

RESOURCE AVAILABILITY

Lead contact

Further information and requests for resources and reagents should be directed to and will be fulfilled by the lead contact (randolph.helfrich@gmail.com).

Materials availability

This study did not generate new unique reagents.

Data and code availability

Freely available software and algorithms used for analysis are listed in the key resources table. All custom code in this manuscript is available upon request from the lead contact. The data is not publicly available given IRB restrictions, but can be obtained through the lead contact.

EXPERIMENTAL MODEL AND SUBJECT DETAILS

Participants

23 healthy older adults (12 males; mean ± SD [range]: 61 ± 14 [21 – 78] years of age, 17 ± 1.5 years of education), 13 patients with lesions in the lateral prefrontal cortex (6 males; 57 ± 9 [41 – 73] years of age; 16 ± 2.5 years of education) and 12 patients with parietal lesions (6 males; 67 ± 21 [20 – 89) years of age, 15 ± 2.6 years of education) were recruited for this study. Lesions were unilateral (PFC: n = 6 left, 7 right hemisphere; PCtx: n = 6 left, 6 right hemisphere; Figure S1A). Participants were selected based on their lesion location. All lesions were chronic (10.43 ± 7.38 [0.74 - 26] years elapsed) and caused by a single stroke or surgical resection of a low-grade tumor. No evidence of tumor regrowth was detected in any of the tumor patients at the time of testing. None of the patients exhibited hemi spatial neglect. Patients were recruited from three different sites. 11 patients were recruited at the University of California, Berkeley, 10 patients were tested at the University of New Mexico's Health Sciences Center, and 3 patients were tested at Oslo University Hospital. Age-matched controls were recruited at the University of California, Berkeley. Two control participants were excluded from the analyses given insufficient EEG data quality (n=1) and excessive drowsiness (n=1). All subjects had normal/corrected-to-normal vision. The patients were evaluated by a clinician prior to testing and had no other neurological or psychiatric diagnoses. All subjects gave informed consent and all procedures were approved by the Institutional Review Board as well as by the Committee for Protection of Human Subjects at the University of California, Berkeley (Protocol number: 2010-02-783) or the Regional Committee for Medical and Healthy Research Ethics and conducted in agreement with the Declaration of Helsinki.

METHOD DETAILS

Lesion reconstruction

Lesion reconstructions were obtained by manual delineation based on structural MRIs (MP-RAGE) obtained after study inclusion under the supervision of a neurologist. Fluid Attenuated Inversion Recovery (FLAIR), T1 and T2 weighted images of each patient's brain were co-registered to a T1 MNI Template using Statistical Parametric Mapping software's (SPM) New Unified Segmentation

Please cite this article in press as: Raposo et al., Periodic attention deficits after frontoparietal lesions provide causal evidence for rhythmic attentional sampling, Current Biology (2023), https://doi.org/10.1016/j.cub.2023.09.065

routine.[79,83] Lesion delineation was then performed on axial mosaics of the normalized T1 scans using MRIcron.[84] The resulting lesion masks were then converted to three-dimensional MNI space using the Mosaic to Volume routine in SPM.

Behavioral task

Stimulus presentation was controlled with EPrime software (Psychology Software Tools). Participants sat ~60 cm away from the screen. They performed a spatial attention reaction time task where they had to maintain fixation on a cross on a dynamic background with several visual distractors (0.11°), which were randomly switched on (visible) or off (invisible) to increase attentional competition. The screen was virtually divided into a Cartesian 7x7 invisible grid and there were 49 potential distractors, each assigned to one of the cells of the grid. With random intervals of 50–250 ms along the trial, one of the distractors was chosen at random and its visibility was switched. Targets never overlapped with distractors. Participants were cued to either the left or right hemifield (left and right cues were randomized) by a centrally presented cue (70% validity) and asked to covertly shift their attention to the cued hemifield. After a variable cue-target interval (1000 – 2000ms), a static blue square target (0.22°) was presented in the center of one of the 49 virtual cells comprising the grid. The target was presented at random intervals within the cue-target interval (in accordance with Helfrich et al.[14]). The target remained on the screen until the subject responded or 2000ms elapsed. Participants were instructed to respond to targets presented in the cued hemifield as quickly as possible and to withhold a response to targets presented in the opposite hemifield. Participants performed the total duration of the task, consisting of 420 trials.

EEG and eye position data acquisition

EEG data were collected using a 64 channel BioSemi ActiveTwo with active electrodes mounted on an elastic cap according to the International 10-20 System (BioSemi, Amsterdam, Netherlands), sampled at 1024 Hz. Vertical electrooculogram (EOG) was recorded with a right inferior eye electrode and a superior eye electrode, and the horizontal EOG was monitored with an electrode at the external canthus. Continuous gaze position was recorded to exclude any trials post hoc where eye movements occurred. Additional eyetracking data were collected at Berkeley and New Mexico using an Eyelink 1000 optical tracker (SR Research, Ontario, Canada), sampled at 1 kHz. No eyetracking was performed in Oslo. Trials that contained eye movements (blinks and/or saccades) based on eye tracking or the EOG were excluded.

QUANTIFICATION AND STATISTICAL ANALYSIS

Behavioral data analysis

We calculated mean target detection accuracy, mean target reaction time and reaction time variance per group. Stimuli were lateralized during presentation, so we further divided patients depending on their lesion location to test for effects of laterality. Spectral analysis on behavioral time courses was performed on the 1000 – 2000 ms cue-target interval after the cue event. Trials where eye movements occurred were excluded and only correct responses to targets at the cued location were considered. To extract the behavioral time-course, we shifted a 50ms window in steps of 1ms from 1000 – 2000ms and re-calculated the reaction times across all validly cued trials in the respective time window. We used relatively long windows of 50ms, which enables frequency estimation up to 20 Hz, in line with previous work (see Helfrich et al.[14]), since some bins did not contain enough trials. To remove any non-numerical values from the data that resulted from the limited temporal sampling, the traces were further smoothed with a 25-point boxcar function, then demeaned and linearly detrended. We obtained spectral estimates from a Fast Fourier Transform (FFT) in steps of 1 Hz from 1 – 20 Hz based on the individual behavioral time course after applying discrete prolate spheroidal sequences (dpss) multi-taper with ±3 Hz spectral smoothing. We attenuated the 1/f background activity by multiplying spectral estimates per frequency-of-interest with the respective center frequency.

EEG data analysis

Preprocessing: The data were offline re-referenced to a common average, de-meaned and linearly detrended, high-pass filtered at 0.3 Hz and low-pass filtered at 70 Hz using finite impulse response filters. Three subjects were originally sampled at 256 Hz and subsequently re-sampled to 1024 Hz. Line noise harmonics (60 Hz for US data and 50 Hz for Oslo data) were removed using a band-stop filter. The data were then visually inspected for artifacts. Eye movements and excessively noisy epochs and channels were rejected. Channels exhibiting increased noise were then reconstructed by interpolation of the mean of the nearest neighboring channels. Next, the data were submitted to an independent component analysis. We excluded components that resembled muscle, heartbeat, or eye movement artifacts (14.9 ± 5.1, mean ± SD). The final dataset included an average of 356 trials per subject (± SD [range] trials: ± 37 [266 – 409]. Finally, the data were epoched into 5 s long segments, starting 1 s before trial onset.

Event-related potentials (ERP): We extracted the ERPs from the epoched data after applying an absolute baseline correction (-0.2 to 0 s before cue onset). The EEG data segments were low-pass filtered at 40 Hz and smoothed with a 30-point boxcar function for display purposes. All correct trials were included.

Spectral analysis: Power spectra were obtained during the cue-target interval. Spectral estimates were computed by means of a FFT after applying a Hanning window (1-40 Hz, 1 Hz steps) and zero padding. We employed IRASA (Irregular Resampling Auto-Spectral Analysis)[35] to disentangle oscillatory activity from concurrent broadband 1/f activity. IRASA estimates were calculated on a 1.5 s time window (from 500ms after cue onset to the end of the cue-target interval), with a moving window of 1 s and a step size of 50 ms. IRASA was calculated per subject, trial and channel. Resampling was performed in a pairwise fashion for factor rf

and the corresponding resampling factor rf* = 2 – r (resampling factors rf: 1.1-1.9 in 0.05 steps). For each window, we calculated the auto-power spectrum by means of a FFT after applying a Hanning window. Then all auto-spectra were median-averaged to obtain the power spectrum of the 1/f component. The 1/f component was subtracted from the original PSD to obtain the oscillatory residuals.

EEG-behavior correlation: Behavior and EEG correlation was computed using a cluster-based correlation between the EEG and the behavior power spectrum from 1 to 20 Hz. Rhythmic behavioral sampling was first averaged within the significant frequency bands (2 – 7 Hz and 12 – 16 Hz) per participant to obtain a single value reflecting behavioral rhythmic sampling. This approach was viable, because rhythmic sampling in the theta and high alpha/low beta bands were not independent (**rho** = 0.6940, $p = 0.0002$). Second, we introduced a composite metric to quantify the dependence of EEG and behavioral power termed rhythmic sampling index (RSI). The index was defined as the vector length (Euclidean distance to the origin of the coordinate system) for every subject, channel, and frequency in a 2D space consisting of normalized (divided by the maximum value) behavior and EEG power. Normalization was necessary to equate the differences in absolute values between the behavioral (ms) and EEG (μV^2) scale.

Phase-behavior correlation: To extract the instantaneous analytic phase, we down-sampled the data to 256 Hz and band-pass filtered the data from 2 – 30 Hz (± center-frequency / 4) per frequency band and applied a Hilbert transform to extract the instantaneous phase at target onset. Only trials where the target was successfully detected were included in the analysis. Next, we binned the phase angles at target onset into 50 equally distributed bins and computed the average phase-resolved reaction times per channel and frequency bin across all trials within a 90° window centered around every phase bin. Subsequently, we determined the phase bin with the slowest RT per participant, channel, and frequency for statistical testing.

Spectrally-resolved voxel-based lesion symptom mapping

Data were further analyzed using an adaptation of voxel-based lesion symptom mapping,[85] which was spectrally-resolved. This method maps the relationship between behavior and brain lesions on a voxel-by-voxel basis. Here, we normalized lesion reconstructions in MNI space for every patient along with their spectrally-resolved behavioral data. The analysis was carried out across all frequencies and subsequently visualized for the behaviorally-relevant frequency ranges (2 – 7 Hz and 12 – 16 Hz) after correction for multiple comparisons across all frequencies and voxels. All lesion maps were flipped onto the left hemisphere to increase statistical power, since we did not observe any differences between lesion hemispheres in all previous analyses. Then, we conducted a *t*-test at every voxel to compare between behavioral power of patients with and without a lesion in that voxel. This approach indexed the brain areas whose damage had the greatest impact on the behavioral power increase in the significant frequency bands. Tests were confined to voxels where there were more than five patients per sub-group (i.e., with and without a lesion). We then z-scored the t-values.

Statistical testing

Throughout, we report single subject data and highlight effects that generalize across the population and were observed in every participant. Unless stated otherwise, we employed two-tailed paired t-tests (Figures 1D, 2C, and 3B) and repeated-measures ANOVA (Figure 2C) to infer significance at the group level. Repeated-measures ANOVA was carried out using the software Jamovi.[82] For the electrophysiological data, we employed cluster-based permutation tests to correct for multiple comparisons as implemented in Fieldtrip (Monte Carlo method; 1000 iterations; 0.05 cluster alpha; 0.025 alpha; maxsum criterion[86]) based on either paired or unpaired two-tailed t-tests, unless stated otherwise. Clusters were either formed in time (e.g., Figure 3A) or in the frequency domain (e.g., Figures 1F, 3D, and 4B). We furthermore used cluster-based correlation based on Pearson correlation coefficient, which was subsequently transformed into a t-statistic (e.g., Figure 4A). We included bootstrapped standard errors where applicable. In several instances where cluster testing was not feasible (e.g., for circular data or voxel-based lesion symptom mapping), we also employed FDR correction (Benjamini-Yekutieli; q = 0.1). Circular statistics as the Rayleigh test and V-test (Figures 4C and 4D), which test for circular non-uniformity and non-uniformity with a specified mean direction respectively, were carried out using the CircStat toolbox.[78] In cases where multiple p-values were obtained (circular data across different dimensions; e.g., frequency and electrodes), we combined p-values using the method by Stouffer et al. to infer significance[87] as outlined in detail by VanRullen.[81] Effect sizes were calculated using Cohen's d, the correlation coefficient rho, or the resultant vector length.